Actuating Eigenmanifolds of Conservative Mechanical Systems Via Bounded or Impulsive Control Actions

Della Santina, C.; Calzolari, Davide; Giordano, Alessandro Massimo; Albu-Schaffer, Alin

DOI
10.1109/LRA.2021.3061391

Publication date
2021

Document Version
Final published version

Published in
IEEE Robotics and Automation Letters

Actuating Eigenmanifolds of Conservative Mechanical Systems via Bounded or Impulsive Control Actions

Cosimo Della Santina, Davide Calzolari, Alessandro Massimo Giordano, and Alin Albu-Schäffer

***Abstract*—Eigenmanifolds are two-dimensional submanifolds of the state space, which generalize linear eigenspaces to nonlinear mechanical systems. Initializing a robot on an Eigenmanifold (or driving it there by control) yields hyper-efficient and regular oscillatory behaviors, called modal oscillations. This letter investigates the possibility of transitioning between two modal oscillations without ever leaving the Eigenmanifold. This is essential to generate control inputs that decrease or increase the amplitude of the nonlinear oscillations. First, we prove that this goal can be achieved using bounded inputs only for Eigenmanifolds with unidimensional projection in configuration space. Then, we show that by allowing for impulsive control actions, the problem can be solved for all Eigenmanifolds which self-intersect when projected in configuration space.**

***Index Terms*—Compliant joints and mechanisms, motion control, natural machine motion.**

I. Introduction

In (ARTICULATED) soft robots, the rigid structure of classic systems is enhanced by introducing purposefully designed elastic elements [1]–[3]. This should give to soft robots the capability of performing regular oscillations with unmatched efficiency. Possible applications range from locomotion to industrial robotics. Indeed, a well-known (and well-understood in the unidimensional or linear cases [4, Secs. II,III]) connection exists between potential fields and oscillations.

Yet, articulated soft robots are not at all simple to control, especially when the desired behavior goes beyond posture regulation [3, Sec. 4.3]. Several general strategies for realizing oscillations in mechanical systems have been recently proposed.

Manuscript received October 15, 2020; accepted February 15, 2021. Date of publication February 23, 2021; date of current version March 17, 2021. This letter was recommended for publication by Associate Editor B. V. Adorno and Editor A.Kheddar upon evaluation of the reviewers' comments. This work was supported by the EU projects 835284 M-Runners and 101016970 NI. *(Corresponding author: Cosimo Della Santina.)*

Cosimo Della Santina is with the Institute of Robotics and Mechatronics, German Aerospace Center (DLR), 82234 Oberpfaffenhofen, Germany, with the Informatics Department, Technical University of Munich (TUM), 85748 Garching bei München, Germany, and also with the Cognitive Robotics Department, 3ME, TU Delft, Delft 2628 CN, Netherlands (e-mail: cosimodellasantina@gmail.com).

Davide Calzolari, Alessandro Massimo Giordano, and Alin Albu-Schäffer are with the Institute of Robotics and Mechatronics, German Aerospace Center (DLR), Oberpfaffenhofen, Germany, and also with the Informatics Department, Technical University of Munich (TUM), 85748 Garching bei München, Germany (e-mail: davide.calzolari@dlr.de; Alessandro.Giordano@dlr.de; Alin.Albu-Schaeffer@dlr.de).

Digital Object Identifier 10.1109/LRA.2021.3061391

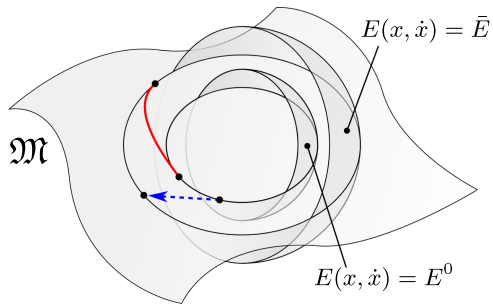

Fig. 1. The orbits of nonlinear modal oscillations of a robot are identified by the intersection of an Eigenmanifold $\mathfrak{M}$ and one level set of $E(x,\dot{x})$. We discuss here control strategies for transitioning from one nonlinear mode to another - i.e. from energy E^0 to energy $\bar{E}$ - without ever leaving the eigenmanifold $\mathfrak{M}$. We prove that this transition can be achieved smoothly (red solid line) only in presence of strong symmetries in the system. We then show that discontinuous jumps (blue dashed arrow) can be achieved for a larger class of systems by using impulsive control actions.

Examples are virtual holonomic constraints in [5], [6], Immersion and Invariance control in [7], and energy shaping in [8]. However, these techniques do not explicitly take into account the benefits of elastic couplings, and may end up with a cancellation by control of the potential forces. Optimal control [9], [10] has been used to explicitly take advantage of elasticity in performing oscillatory tasks, but it is necessarily tailored on low dimensional robots and specific tasks. Finally, several works combined model matching, bio-mechanical inspiration, and engineering intuition, yielding very promising results within specific tasks and hardware platforms [11]–[14]. Nevertheless, these strategies only partially exploit the intrinsic dynamics of the robot, since they are still based on (partial) dynamics cancellation.

An alternative solution can be found in nonlinear modal theory. This is a thriving research area [4], [15] aiming at extending linear modal analysis to the nonlinear domain. Within this context, Eigenmanifolds are defined as a curved counterpart of linear eigenspaces. An Eigenmanifold describes a family of periodic orbits (modal oscillations) that the robot can perform as open loop evolutions. Each trajectory is characterized by a distinct energy level. The concept is used for control purposes in [16], where it is shown that making an Eigenmanifold a local attractor by means of feedback control is a simple way of exciting hyper-efficient nonlinear oscillations in robotic systems.

Yet, assuring that the system state converges to the Eigenmanifold is not enough, because there are infinite modal oscillations in an Eigenmanifold. An additional problem which

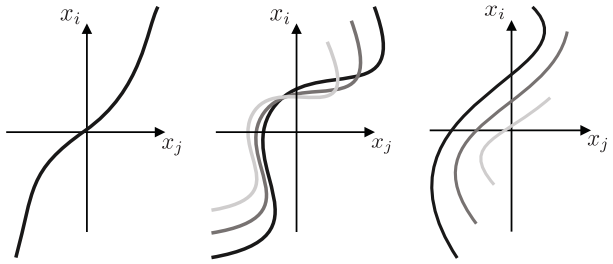

(a) One dimension (b) Self-intersect (c) Not self-intersect

Fig. 2. Whenever an Eigenmanifold is projected in configuration space (i.e. the velocity part is not considered) one of three things can happen. We provide here illustrative examples, by singling three modes out of the whole manifold projection. If the system is equipped with strong symmetries, then all the trajectories can be part of a one dimensional manifold, as shown in Panel (a). More commonly, the trajectories may stay close and intersect with each others, as in Panel (b). Finally, the trajectories may spread out, and do not intersect each other, as in Panel (c).

needs to be addressed is the regulation of a specific mode, which corresponds to a desired behavior. This problem was not addressed in previous work[1] and it is the subject of the present paper (Fig. 1). We analyze in which extent we can act upon a system that is evolving on an Eigenmanifold, without having it exiting this relevant region of the state space. First, we prove that Eigenmanifolds that can be actuated with bounded control actions must be equipped with strong symmetries (see Fig. 2(a)). We then extend our range of investigation to impulsive actions, i.e. unbounded inputs with bounded energy. Impulsive control theory finds application in many fields, including financial trading [17], epidemics [18], and astronautical science [19]. The use of impulsive controllers to stabilize periodic motions in linear systems is summarized in [20, Chs. 9,10]. We show that by allowing for impulses, Eigenmanifolds with a more general structure can be actuated (see Fig. 2(b)). For both cases, we provide control algorithms bringing the system to the desired energy level without ever exiting the Eigenmanifold.

A. Notation

This work deals with nonlinear conservative mechanical systems that can be described by the standard form $M(x)\ddot{x} + C(x,\dot{x})\dot{x} + \partial V(x)/\partial x = \tau$, where $x \in \mathbb{R}^n$ are the configuration coordinates of the robot, with time derivatives $\dot{x}, \ddot{x}$. The state is $(x,\dot{x}) \in \mathbb{R}^{2n}$. The configuration dependent inertia matrix is $M(x) \in \mathbb{R}^{n\times n}$, and $C(x,\dot{x}) \in \mathbb{R}^{n\times n}$ collects Coriolis and centrifugal terms. The potential function is $V(x) \in \mathbb{R}$, and it possibly includes gravity and elastic contributions. In this letter we assume V to be positive definite and radially unbounded. This in turn implies that its level curves are closed. The total energy is $E(x,\dot{x}) = \frac{1}{2}\dot{x}^{\mathrm{T}} M(x)\dot{x} + V(x)$. $x_{\mathrm{eq}} \in \mathbb{R}^n$ is a minimum of V, i.e. an equilibrium of the system. Finally, $\tau \in \mathbb{R}^n$ is the control input. Hence, the system is fully actuated and it is not subject to non-holonomic constraints. In the following, with bounded input (or action) we mean that $\tau < \infty$ for all $||(x,\dot{x})|| < \infty$.

II. Eigenmanifolds in a Nutshell

This section provides a short and operative introduction to Eigenmanifolds, without any claims of exhaustiveness. The reader interested in knowing more about the mathematically accurate definition and its properties can find them in [4, Sec. 7]. Moving from the linear to the nonlinear case, the eigenspace ES (which geometrically is a plane) bends into a curved surface of dimension 2, which we characterize with the following definition. Consider the system in Sec. I-A with $\tau = 0$. We say that a 2-dimensional submanifold $\mathfrak{M}$ of the state space $\mathbb{R}^{2n}$ is an Eigenmanifold if

i) it contains the equilibrium, i.e. $(x_{\mathrm{eq}}, 0) \in \mathfrak{M}$,
ii) it is a collection of periodic orbits characterized by a distinct energy - i.e. each $x(t)$ such that $(x(0),\dot{x}(0)) \in \mathfrak{M}$ is periodic, it is fully contained in $\mathfrak{M}$, and have a total energy E distinct from all other trajectories in $\mathfrak{M}$,
iii) all these orbits are line-shaped - i.e. they are homeomorphic to a segment when projected in configuration space. Examples are provided in Fig. 2.

Thus, each Eigenmanifold characterizes a family of regular, oscillatory, and autonomous behaviors, which grows continuously from an equilibrium.

Suppose that ES is an eigenspace of the linearized system at the equilibrium point x_{eq}, which is also tangent to the Eigenmanifold. In this case, we say that $\mathfrak{M}$ is the continuation of ES. As discussed in [4, Sec. 9], two functions $X : ES \to \mathbb{R}^n$ and $\dot{X} : ES \to \mathbb{R}^n$ - called *coordinate expression of the Eigenmanifold embedding* - can always be found so that the Eigenmanifold can be (locally) defined in coordinates as

$$\mathfrak{M} = \left\{(x,\dot{x}) \in \mathbb{R}^{2n},\ \text{s.t.}\ X(x_{\mathrm{m}},\dot{x}_{\mathrm{m}}) = x, \dot{X}(x_{\mathrm{m}},\dot{x}_{\mathrm{m}}) = \dot{x}\right\},$$

where $(x_{\mathrm{m}},\dot{x}_{\mathrm{m}}) \in \mathbb{R}^2$ are the coordinates of the eigenspace ES defined above. We assume the Jacobian of $(X,\dot{X}) - (x,\dot{x})$ to have everywhere the maximum rank possible.

III. Problem Statement

Two complementary control challenges can be identified, which if simultaneously addressed can lead to an effective regulation of modal oscillations [16]

c1) *Eigenmanifold stabilization*, i.e. finding a closed loop $\tau_{\mathrm{c1}}(x,\dot{x},t)$ such that $\mathfrak{M}$ is asymptotically stable.[2]
c2) *Eigenmanifold actuation*, i.e. finding a closed loop $\tau_{\mathrm{c2}}(x,\dot{x},t)$ such that $E(x(\infty),\dot{x}(\infty)) = \bar{E}$, for any given $\bar{E}$. This challenge is summarized by Fig. 1.

Regarding (c2), note that there is a unique relation between modes and energy on the Eigenmanifold - as expressed by (ii) in Sec. II. Therefore, we can reason in terms of energy instead of configurations or specific trajectories.

We consider the goals (c1) and (c2) to be implemented by separate loops acting in parallel, i.e. $\tau = \tau_{\mathrm{c1}} + \tau_{\mathrm{c2}}$. In the general case, the two loops may interact with each other, making quite hard to formally asses any convergence property. Also, this may not be efficient, since one can counteract the other. We therefore introduce the following decoupling conditions, aimed at assuring that the two controllers do not act simultaneously. The conditions are

$$\tau_{\mathrm{c1}}(x,\dot{x},t) = 0,\ \forall t \in \mathbb{R},\ \forall (x,\dot{x}) \in \mathfrak{M}, \tag{1}$$

and

$$(x(0),\dot{x}(0)) \in \mathfrak{M}\ \Rightarrow (x(t),\dot{x}(t)) \in \mathfrak{M}, \forall\, t > 0. \tag{2}$$

[1] In [16] we stated the challenge, and provided a preliminary heuristic for proof of concept purposes.

[2] See [21] for the definition of asymptotically stable sets.

Note that if (1) holds, then (2) is a condition on τ_{c2} only. If τ verifies this condition, we say that it *preserves* $\mathfrak{M}$. If this is the case, then the closed loop system still has a manifold $\mathfrak{M}$ which verifies (i) and (ii). We do not care about avoiding self intersections during actuation - i.e. condition (iii). If additionally τ_{c1} converges in finite time then the asymptotic stability of the whole closed loop is trivially implied. Otherwise, it requires arguments as in [21].

This letter investigates the design of τ_{c2}. Therefore, we assume that $(x(0), \dot{x}(0)) \in \mathfrak{M}$, and that τ_{c1} is such that (1) holds (see for example [16, Sec. III]). In this case $\tau = \tau_{c2}$, and as such we omit the subscript. The aim is therefore to find a τ_{c2} such that (c2) is achieved, and (2) is verified. First we consider the bounded case. This is the standard kind of actuation that is typically of robotics, but it proves to be quite limited to solve the problem at hand. We discuss it in Sec. IV. Then, we deal with Eigenmanifold actuation through impulsive actions in Sec. V.

A. Impulsive Inputs

We define an impulsive input as [20]

$$u^* \delta(t - t^*) \tag{3}$$

where $\delta(t - t^*)$ is the Dirac's delta centered in t^* and of unitary integral, and $u^* \in \mathbb{R}^n$ is a constant vector distributing the impulse in the n directions. Note that a perfect δ cannot be implement in the practice. Instead, (3) has proven to be a good model of an high amplitude action delivered in a very short time [19], [20], [22]. Discussing robustness issues which may be associated to this abstraction is beyond the scope of the present paper. Thanks to the delta's sampling property, the effect of taking τ equal to (3) is the following abrupt change of state (jump hereinafter)

$$(x, \dot{x}) \mapsto (x, \dot{x} + M^{-1}(x) u^*). \tag{4}$$

This corresponds to a change of energy equal to $||\dot{x} + M^{-1}(x)u^*||_{\mathrm{M}} - ||\dot{x}||_{\mathrm{M}}$, where $||\cdot||_{\mathrm{M}}$ is the norm induced by the metric tensor $M(x)$. We refer to modal coordinates prior to the jump as $(x_{\mathrm{m}}^-, \dot{x}_{\mathrm{m}}^-) \in \mathbb{R}^2$ such that

$$\lim_{t \to (t^*)^-} (x(t), \dot{x}(t)) = \left(X(x_{\mathrm{m}}^-, \dot{x}_{\mathrm{m}}^-), \dot{X}(x_{\mathrm{m}}^-, \dot{x}_{\mathrm{m}}^-) \right). \tag{5}$$

Similarly, $\dot{x}_{\mathrm{m}}^+$ is the right limit of $\dot{x}_{\mathrm{m}}$ in t^*.

IV. Bounded Control Action

In this section we assume that the modal coordinates are one of the robot's configurations and its derivative - that is $(x_{\mathrm{m}}, \dot{x}_{\mathrm{m}}) = (x_i, \dot{x}_i)$ for some $i \in \{1 \dots n\}$. This is done for the sake of clarity of notation, and wlog.

Theorem 1: If $X \in C^\infty$, $\tau < \infty$ for all $||(x, \dot{x})|| < \infty$, and $||\tau|| \neq 0$, then τ preserves $\mathfrak{M}$ if and only if $\partial X / \partial \dot{x}_i \equiv 0$.

Proof: Condition (ii) in Sec. II can be reformulated in terms of the embedding as $\mathrm{d}((x, \dot{x}) - (X, \dot{X}))/\mathrm{d}t|_{(x,\dot{x}) \in \mathfrak{M}} = 0$. This in turn is equivalent (see [16, Sec. III-C]) of asking that $(X, \dot{X})$ verifies the PDEs $\forall j \in \{1 \dots n\}$

$$\dot{X}_j - \frac{\partial X_j}{\partial x_i} \dot{x}_i - \frac{\partial X_j}{\partial \dot{x}_i} f_i(X, \dot{X}) = 0, \tag{6}$$

$$f_j(X, \dot{X}) - \frac{\partial \dot{X}_j}{\partial x_i} \dot{x}_i - \frac{\partial \dot{X}_j}{\partial \dot{x}_i} f_i(X, \dot{X}) = 0, \tag{7}$$

where $f(x, \dot{x}) = -M^{-1}(x)(C(x, \dot{x})\dot{x} + \frac{\partial V(x)}{\partial x})$, and the index j identifies $j-$th component of the vector. The case $i = j$ is trivially verified. Thus we assume $i \neq j$ hereinafter.

If $\tau(x, \dot{x}, t) < \infty$ is such that it does not push the system out of the manifold, it must verify (6) and (7) with $f(x, \dot{x})$ replaced by $f(x, \dot{x}) + M^{-1}(x)\tau(x, \dot{x}, t)$, and still $(x, \dot{x}) = (X, \dot{X})$. Subtracting the PDEs with and without actuation yields the orthogonality constraints $\forall j \neq i$

$$\left(\frac{\partial X_j}{\partial \dot{x}_i} M_i^{-1} \right) \tau = 0, \quad \left(M_j^{-1} - \frac{\partial \dot{X}_j}{\partial \dot{x}_i} M_i^{-1} \right) \tau = 0, \tag{8}$$

where M_i^{-1} and M_j^{-1} are the $i-$th and $j-$th rows of M^{-1} respectively. We assume now *ad absurdum* that it exists at least a j such that $\partial X_j / \partial \dot{x}_i \neq 0$ for which (8) is verified with $\tau \neq 0$. If this is the case, we can multiply the constraints on the left hand side of (8) by $(\partial \dot{X}_j / \partial \dot{x}_i)/(\partial X_j / \partial \dot{x}_i)$. Then, we can add the result to the constraints on the right hand side of (8). This yields the following equivalent condition

$$\mathrm{Rank} \left\{ \frac{\partial X_1}{\partial \dot{x}_i} M_i^{-1} \dots, \frac{\partial X_{i-1}}{\partial \dot{x}_i} M_i^{-1}, \frac{\partial X_{i+1}}{\partial \dot{x}_i} M_i^{-1} \dots, \frac{\partial X_n}{\partial \dot{x}_i} M_i^{-1}, M_1^{-1} \dots, M_{i-1}^{-1}, M_{i+1}^{-1} \dots M_n^{-1} \right\} < n$$

Note that $\partial X_j / \partial \dot{x}_i$ is a scalar. Therefore, the first $n - 1$ vectors are linearly dependent. Thus, their contribution can be described by a single vector pointing in the same direction

$$\mathrm{Rank} \left\{ M_1^{-1} \dots, M_{i-1}^{-1}, \left|\left| \frac{\partial X}{\partial \dot{x}_i} \right|\right| M_i^{-1}, M_{i+1}^{-1} \dots M_n^{-1} \right\} < n. \tag{9}$$

Since M^{-1} is full rank, this condition is fulfilled if and only if $\partial X / \partial \dot{x}_i = 0$, which leads to an *absurdum*. Therefore, τ can be different from zero only when $\partial X / \partial \dot{x}_i = 0$. This is however a point-wise property. We must now make it global. Since X is smooth by hypothesis, it can either be zero in a set of isolated points, or everywhere. The first case is of no use, since a $\tau < \infty$ which is different from zero only on a set with null measure does not modify the state evolution. The latter case yields the only-if part of the theorem.

The if part is proven by considering that the right hand side of (8) identifies $n - 1$ orthogonality constraints in dimension n. Therefore, there is always at least one direction in which τ can be exerted without violating the constraints. ■

Remark 1: Condition $\partial X / \partial \dot{x}_i \equiv 0$ is purely geometric. It requires that the projection of $\mathfrak{M}$ in the configuration space (which in coordinates means to drop the $\dot{x}$ component of the state) is a manifold of dimension one. This scenario is portrayed in Fig. 2(a). In our previous work [23] we have proven that this can happen only if kinetic energy is constant along the trajectories of $M(x)\ddot{x} + C(x, \dot{x})\dot{x} = 0$ contained in the projection of $\mathfrak{M}$.

Lemma 1: If $\dot{X} \in C^\infty$ and $\partial X / \partial \dot{x}_i \equiv 0$, then $\tau = M(x)(\partial X / \partial x_i)\tau^*$ is a manifold preserving action $\forall \tau^* \in \mathbb{R}$.

Proof: Eq. (8) becomes

$$\left(M_j^{-1} - \frac{\partial \dot{X}_j}{\partial \dot{x}_i} M_i^{-1} \right) M \frac{\partial X}{\partial x_i} \tau^* = 0. \tag{10}$$

Note now that $M_j^{-1} M$ is the row vector having all null elements, except for the $j-$th that is one. Also, consider that by definition

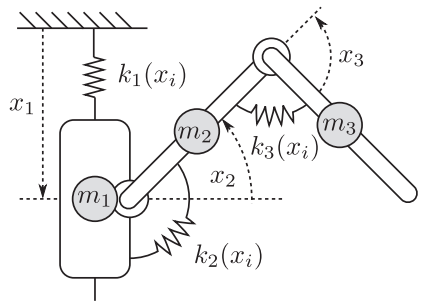

Fig. 3. PRR planar manipulator, with parallel elasticity at each joint. For opportune choice of the stiffness characteristics, one of the Eigenmanifolds of the robot has one dimensional projection in configuration space - i.e. it is a strict mode.

$(\partial X_i/\partial x_i) = 1$. Therefore (10) becomes

$$\left(\frac{\partial X_j}{\partial x_i} - \frac{\partial \dot{X}_j}{\partial \dot{x}_i}\right)\tau^* = 0. \tag{11}$$

This condition is fulfilled for all τ^*. Indeed, according to (6) if $\partial X/\partial \dot{x}_i \equiv 0$ then $\dot{X}_j = (\partial X_j/\partial x_i)\dot{x}_i$. Thus,

$$\frac{\partial \dot{X}_j}{\partial \dot{x}_i} = \frac{\partial^2 X_j}{\partial x_i \partial \dot{x}_i}\dot{x}_i + \frac{\partial X_j}{\partial x_i} \;\Rightarrow\; \frac{\partial \dot{X}_j}{\partial \dot{x}_i} = \frac{\partial X_j}{\partial x_i},$$

where we exploited the holonomicity of X. ■

Therefore, if $\mathfrak{M}$ is strict, we always have the freedom of imposing a one dimensional feedback action τ^*, by making it tangent to the manifold. Note that Lemma 1 is coherent with [23, Theorem 1]. We use this result to derive a manifold preserving controller that injects or removes energy from the system.

A. Control Strategy

Consider the following control action for on-manifold energy regulation

$$\tau = \gamma(\bar{E} - E)M(x)\dot{x} \tag{12}$$

where $\bar{E}$ is the desired level of energy to be reached, and $\gamma > 0$ is a control gain.

Corollary 1: Under the hypotheses of Lemma 1, and if $(x(0), \dot{x}(0)) \in \mathfrak{M}$, then (12) is such that $(x(t), \dot{x}(t)) \in \mathfrak{M}$ for all $t > 0$. Furthermore, if $(x(0), \dot{x}(0)) \neq (x_{\text{eq}}, 0)$ then $E \to \bar{E}$ for $t \to \infty$.

Proof: Consider that, if $(x(t), \dot{x}(t)) \in \mathfrak{M}$ and $\partial X/\partial \dot{x}_i \equiv 0$, from (6), then $\dot{X}_j = (\partial X_j/\partial x_i)\dot{x}_i$. Thus, (12) becomes $\tau = \gamma(\bar{E} - E)M(x)(\partial X/\partial x_i)\dot{x}_i$, which is equivalent to what prescribed by Lemma 1 for $\tau^* = \gamma(\bar{E} - E)\dot{x}$. This concludes the innovative part of the proof. The second part follows standard steps in energy regulation, which we only sketch. First, we evaluate the variation of energy $\dot{E} = \gamma(\bar{E} - E)||\partial X/\partial x_i||^2 \dot{x}_i^2$. Then, we use Barbalat's Lemma with Lyapunov candidate $(\bar{E} - E)^2/2$. This yields that the energy converges either to $\bar{E}$, or to $E(x_{\text{eq}}, 0)$. The latter is excluded through local linear analysis. ■

B. Simulations

We consider the system depicted in Fig. 3 with potential energy $V(X(x_{\text{m}})) = \frac{1}{2}kx_{\text{m}}^2$, with $k > 0$, $x_{\text{m}} = 0.53x_1 + 0.66x_2 + 0.53x_3$, and perform simulations on the strict mode

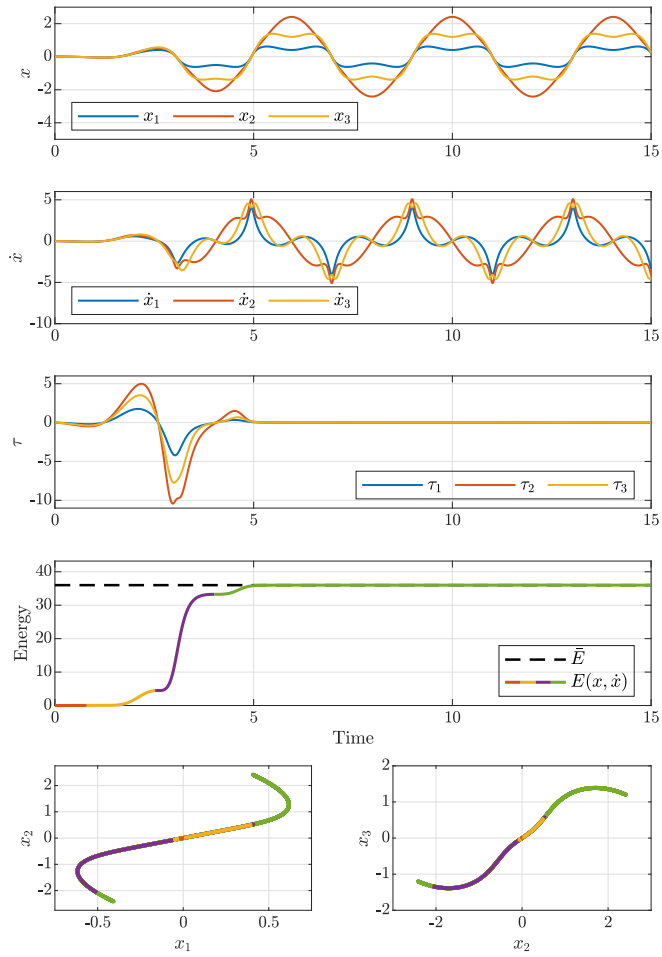

Fig. 4. Plots showing the regulation of the energy $E(x, \dot{x})$ to the desired value $\bar{E} = 36$ with gain $\gamma = 0.1$, and the relative evolution of state along the strict mode in configuration space.

discussed in [23], using (12) to achieve a desired level of energy. The starting configuration is on the mode, close to the equilibrium. The resulting evolutions of the energy and of the state along the mode are presented in Fig. 4, together with the system trajectories and input torques. The desired energy level is reached in few seconds, with bounded control actions, and without ever exiting $\mathfrak{M}$. Also the control action converges to zero as soon as the energy is close to $\bar{E}$.

V. Impulsive Control Action

The following Lemma aims at completely characterizing the kind of impulsive actions that can be produced in an Eigenmanifold preserving fashion, i.e. without ever leaving the manifold.

Lemma 2: An Eigenmanifold $\mathfrak{M}$ admits an impulsive action (3) verifying (2) if and only if for some $\dot{x}_{\text{m}}^+ \in \mathbb{R}$

$$X(x_{\text{m}}^-, \dot{x}_{\text{m}}^-) = X(x_{\text{m}}^-, \dot{x}_{\text{m}}^+), \tag{13}$$

where $(x_{\text{m}}^-, \dot{x}_{\text{m}}^-)$ is as in (5). In this case, the state $(X(x_{\text{m}}^-, \dot{x}_{\text{m}}^+), \dot{X}(x_{\text{m}}^-, \dot{x}_{\text{m}}^+))$ is reached using the impulse

$$u^*(x, \dot{x}) = M(x)(\dot{X}(x_{\text{m}}^-, \dot{x}_{\text{m}}^+) - \dot{X}(x_{\text{m}}^-, \dot{x}_{\text{m}}^-)), \tag{14}$$

which is therefore a manifold preserving control action.

Algorithm 1: Singlejump$(E^0, \bar{E})$.

1: **for all** $\psi \in [-\pi, \pi]$ **do**
2: $\hat{v} \leftarrow (\cos(\psi), \sin(\psi))$
3: $d \leftarrow \arg\min_{\Delta>0}(E(X(\Delta\hat{v}), \dot{X}(\Delta\hat{v})) - E^0)^2$
4: $(x_{\mathrm{m}}^-, \dot{x}_{\mathrm{m}}^-) \leftarrow d\hat{v}$
5: $M^- \leftarrow M(X(x_{\mathrm{m}}^-, \dot{x}_{\mathrm{m}}^-))$
6: $c \leftarrow 2(\bar{E} - E^0) + ||\dot{X}(x_{\mathrm{m}}^-, \dot{x}_{\mathrm{m}}^-)||^2_{M^-}$
7: $\dot{x}_{\mathrm{m}}^+ \leftarrow \arg\min_{\dot{\xi}\in\mathbb{R}}(||\dot{X}(x_{\mathrm{m}}^-, \dot{\xi})||^2_{M^-} - c)^2$
8: $u^* \leftarrow M^-(\dot{X}(x_{\mathrm{m}}^-, \dot{x}_{\mathrm{m}}^+) - \dot{X}(x_{\mathrm{m}}^-, \dot{x}_{\mathrm{m}}^-))$
9: **if** $||X(x_{\mathrm{m}}^-, \dot{x}_{\mathrm{m}}^+) - X(x_{\mathrm{m}}^-, \dot{x}_{\mathrm{m}}^-)|| < \epsilon$ **then**
10: **return** $(x_{\mathrm{m}}^-, \dot{x}_{\mathrm{m}}^-, \dot{x}_{\mathrm{m}}^+, u^*)$
11: **return** Null

Proof: If (2) holds, then the state reached by the system after the jump is part of the Eigenmanifold. We can therefore express it in modal coordinates as $(X(x_{\mathrm{m}}^+, \dot{x}_{\mathrm{m}}^+), \dot{X}(x_{\mathrm{m}}^+, \dot{x}_{\mathrm{m}}^+))$, with $(x_{\mathrm{m}}^+, \dot{x}_{\mathrm{m}}^+) \in \mathbb{R}^2$. However, according to (4) the state before and after the jump must share the same configuration. Since the entire configuration cannot change, also x_{m} must remain the same. Thus, the jump in modal coordinates is $(x_{\mathrm{m}}^-, \dot{x}_{\mathrm{m}}^-) \mapsto (x_{\mathrm{m}}^-, \dot{x}_{\mathrm{m}}^+)$, which yields the state update

$$\left(X(x_{\mathrm{m}}^-, \dot{x}_{\mathrm{m}}^-), \dot{X}(x_{\mathrm{m}}^-, \dot{x}_{\mathrm{m}}^-)\right) \mapsto \left(X(x_{\mathrm{m}}^-, \dot{x}_{\mathrm{m}}^+), \dot{X}(x_{\mathrm{m}}^-, \dot{x}_{\mathrm{m}}^+)\right). \tag{15}$$

Eq. (13) must hold in order for (15) to be compatible with (4). Note that all these steps hold in both directions, so both if and only if implications are proved. Finally, in (4), substitute $\dot{x}$ with $\dot{X}(x_{\mathrm{m}}^-, \dot{x}_{\mathrm{m}}^-)$ and $\dot{x} + M^{-1}u^*$ with $\dot{X}(x_{\mathrm{m}}^-, \dot{x}_{\mathrm{m}}^+)$. Making u^* explicit directly leads to (14). ■

Remark 2: Eq. (13) is purely geometric as well. It indeed requires that the projection of $\mathfrak{M}$ in configuration space self-intersects in x_{m}. In other words, there are at least two modes passing though x_{m}. This scenario is portrayed in Fig. 2(b). Thus, (13) directly generalizes the holonomicity condition $\partial X/\partial \dot{x}_i \equiv 0$ discussed in Sec. IV.

As of now Eigenmanifolds are defined under the assumption of non-hybrid and conservative dynamics [4].

Yet, we believe that this letter already provides some useful insights on how to drop these assumptions. We envision that the controllers proposed in Sec. IV-A and in the next sections can compensate for energy loss. More importantly, Lemma 2 can be seen as defining necessary and sufficient conditions under which a robot maintains its Eigenmanifolds when subject to external impacts (e.g. locomotion).

A. Reachability by Timing and Combining Impulses

We refer to jumping as the process of changing configuration within an Eigenmanifold under the action of (14). Consider an initial configuration $\{(x_{\mathrm{m}}(0), \dot{x}_{\mathrm{m}}(0))\} \in \mathcal{P}(\mathbb{R}^2)$, where the latter is the power set of the real plane - i.e. the set of all possible subsets of $\mathbb{R}^2$. Based on the results discussed in the previous subsection, we can define an operator $\mathcal{J} : \mathcal{P}(\mathbb{R}^2) \to \mathcal{P}(\mathbb{R}^2)$ that extracts all points that can be reached through one jump

$$\mathcal{J} : \mathcal{S} \mapsto \Big\{(\xi, \dot{\xi}) \in \mathbb{R}^2 \mid \exists (\xi, \dot{\xi}^-) \in \mathcal{S} \text{ s.t. } X(\xi, \dot{\xi}^-) = X(\xi, \dot{\xi})\Big\}. \tag{16}$$

Yet, $\mathcal{J} \circ \{(x_{\mathrm{m}}(0), \dot{x}_{\mathrm{m}}(0))\}$ does not take into account that we are not compelled to jump right away, i.e. it is forcing $t^* = 0$. Moving t^* towards strictly positive values is equivalent to include in $\mathcal{S}$ all the possible configurations that can be reached as open loop evolution of the system. This in general could be represented through forward integration, which however cannot be evaluated in closed form. Instead, we exploit here the fact that the system is supposed to evolve on the Eigenmanifold. Its evolution is therefore a modal oscillation with constant and distinct energy. This means that timing the impulse corresponds to selecting $(x, \dot{x})$ from a one dimensional manifold. Then, we define a further operator $\mathcal{W} : \mathcal{P}(\mathbb{R}^2) \to \mathcal{P}(\mathbb{R}^2)$ that extracts all modal states that can be reached as an open loop evolution

$$\mathcal{W} : \mathcal{S} \mapsto \Big\{(\xi, \dot{\xi}) \in \mathbb{R}^2 \mid \exists (\xi^0, \dot{\xi}^0) \in \mathcal{S} \text{ s.t. } E(\xi^0, \dot{\xi}^0) = E(\xi, \dot{\xi})\Big\}. \tag{17}$$

Note that $\mathcal{J} \circ \mathcal{J} = \mathcal{J}$ and $\mathcal{W} \circ \mathcal{W} = \mathcal{W}$, as expected when considering the associative nature of the forward integration operator, and of (3). Instead $\mathcal{J} \subseteq \mathcal{J} \circ \mathcal{W}$. Along the same line we can combine multiple sequences of jumps and waitings yielding to the operator

$$(\mathcal{J} \circ \mathcal{W})^k = \underbrace{(\mathcal{J} \circ \mathcal{W}) \circ \cdots \circ (\mathcal{J} \circ \mathcal{W})}\, k \text{ times}, \tag{18}$$

where $(\mathcal{J} \circ \mathcal{W})^{k-1} \subseteq (\mathcal{J} \circ \mathcal{W})^k$. This in terms of inputs corresponds to an impulse train, with each delta opportunely distanced and scaled. To conclude, the set of reachable modal states from the initial modal coordinates $(x_{\mathrm{m}}^0, \dot{x}_{\mathrm{m}}^0)$ is

$$\mathcal{R}^k = (\mathcal{J} \circ \mathcal{W})^k \circ \left\{(x_{\mathrm{m}}^0, \dot{x}_{\mathrm{m}}^0)\right\}, \quad \mathcal{R} = \lim_{k\to\infty} \mathcal{R}^k. \tag{19}$$

Therefore the Eigenmanifold is fully reachable if $\mathcal{R} = \mathbb{R}^2$. Note that this definition fully exploits the structure of the problem at hand, and it is therefore different from standard controllability by impulses [20, Def. 2.3.1]. Among other things, the analysis is always performed in a space of dimension 2, no matter how large n is.

B. A Control Strategy Exploring $\mathcal{R}^1$

Algorithm 1 evaluates the timing (in the form of the pre-jumping modal coordinates $x_{\mathrm{m}}^-, \dot{x}_{\mathrm{m}}^-$) and the amplitude of a jump u^*, to get from an initial condition $(x(0), \dot{x}(0)) \in \mathfrak{M}$ with energy E^0 to a desired energy level $\bar{E}$. This is done by performing an exhaustive exploration of $\mathcal{W} \circ \{(x_{\mathrm{m}}(0), \dot{x}_{\mathrm{m}}(0))\}$, in search for a good point from where to produce a jump reaching the desired energy level . This idea is sketched in Fig. 5. The following Lemma assesses the validity of the proposed strategy.

Lemma 3: If $(x_{\mathrm{m}}^-, \dot{x}_{\mathrm{m}}^+) \in \mathcal{R}^1$ exists such that $E(x_{\mathrm{m}}^-, \dot{x}_{\mathrm{m}}^+) = \bar{E}$, then Algorithm 1 will find it and produce a correct output.

Proof: Modal orbits are closed and they encompass the origin (0,0). Therefore, for each unit vector $\hat{v} = (\cos(\psi), \sin(\psi))$ there can be only one scaling factor d such that $d\hat{v}$ is contained in $\mathcal{W} \circ \{(x_{\mathrm{m}}(0), \dot{x}_{\mathrm{m}}(0))\}$. Otherwise this would mean that there are portions of the orbit such that the change of x_{m} and the sign of $\dot{x}_{\mathrm{m}}$ are not coherent. The value d can be taken as the one producing the correct energy E^0 - as done in line 3. On the other hand, the closeness of the orbits in $\mathbb{R}^2$ yields through basic topological arguments that each $\psi \in [-\pi, \pi]$ corresponds to at

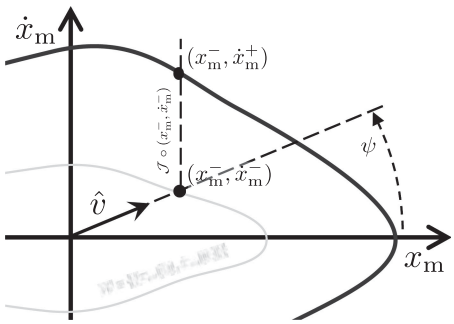

Fig. 5. A visual representation of the key steps performed by Algorithm 1, with salient quantities highlighted. The light gray solid line is pre-jump mode, while the dark gray one is the post-jump mode.

Algorithm 2: Multiplejumpsmontecarlo$(E^0, \bar{E}, k)$.

1: **do**
2: $i \leftarrow 1$
3: **do**
4: **if** $i < k$ **then**
5: $\bar{E}^i \leftarrow \mathrm{normal}(E^0)$
6: **else**
7: $\bar{E}^k \leftarrow \bar{E}$
8: $(x_{\mathrm{m}}^i, \dot{x}_{\mathrm{m}}^i, \dot{x}_{\mathrm{m}}^+, u^{*,i}) \leftarrow \mathrm{oneJump}(x_{\mathrm{m}}^{i-1}, \dot{x}_{\mathrm{m}}^+, \bar{E}^i)$
9: $i \leftarrow i + 1$
10: **while** $i \leq k$ **and** $\mathrm{isNotNull}(x_{\mathrm{m}}^i, \dot{x}_{\mathrm{m}}^i, \dot{x}_{\mathrm{m}}^+, u^{*,i})$
11: **while** $\mathrm{isNotNull}(x_{\mathrm{m}}^i, \dot{x}_{\mathrm{m}}^i, \dot{x}_{\mathrm{m}}^+, u^{*,i})$
12: **Return** $(x_{\mathrm{m}}^1, \dot{x}_{\mathrm{m}}^1, u^{*,1}) \dots (x_{\mathrm{m}}^m, \dot{x}_{\mathrm{m}}^m, u^{*,m})$

least one element of the set. Thus, lines 1 to 4 evaluate all and only the elements of $\mathcal{W} \circ \{(x_{\mathrm{m}}(0), \dot{x}_{\mathrm{m}}(0))\}$ such that $\dot{x}_{\mathrm{m}}^- \geq 0$.

The second part of the for loop (starting from line 5), attempts to produce a feasible jump starting from the state with phase ψ. Such a jump should lead to a $\dot{x}_{\mathrm{m}}^+$ yielding the right energy level $\bar{E}$, and verify condition (13) - i.e. be part of the image of $\mathcal{J}$. The latter is directly verified at line 9. So, for assessing the former we can assume that this is true.

Thus, the condition can be rewritten as $\bar{E} = E(X(x_{\mathrm{m}}^-, \dot{x}_{\mathrm{m}}^-), \dot{X}(x_{\mathrm{m}}^-, \dot{x}_{\mathrm{m}}^+))$. We now subtract the expression for E^0 yielding

$$\bar{E} - E^0 = \frac{1}{2}\left(||\dot{X}(x_{\mathrm{m}}^-, \dot{x}_{\mathrm{m}}^+)||_{M^-} - \dot{X}(x_{\mathrm{m}}^-, \dot{x}_{\mathrm{m}}^-)||_{M^-}\right), \quad (20)$$

where $||\cdot||_{M^-}^2$ is the norm weighted on $M^- = M(X(x_{\mathrm{m}}^-, \dot{x}_{\mathrm{m}}^-))$. Lines 5 to 7 are a direct translation of (20). Thus, Algorithm 1 is equivalent to an exhaustive search of $\mathcal{J} \circ \mathcal{W} \circ \{(x_{\mathrm{m}}(0), \dot{x}_{\mathrm{m}}(0))\} = \mathcal{R}^1$. This concludes the proof. ■

Algorithm 1 contains two nonlinear optimizations, which however are convex. The proof of this statement is not provided here for the sake of space. It is also important to recognize that Algorithm 1 may seem to require spanning all the possible values of ψ continuously. Random sampling or gridding can be considered as solutions. Alternatively, we can consider that the loop is formally equivalent to finding a ψ which solves $X(x_{\mathrm{m}}^-(\psi), \dot{x}_{\mathrm{m}}^+(\psi)) - X(x_{\mathrm{m}}^-(\psi), \dot{x}_{\mathrm{m}}^-(\psi)) = 0$. This value can be found using a standard bisection algorithm.

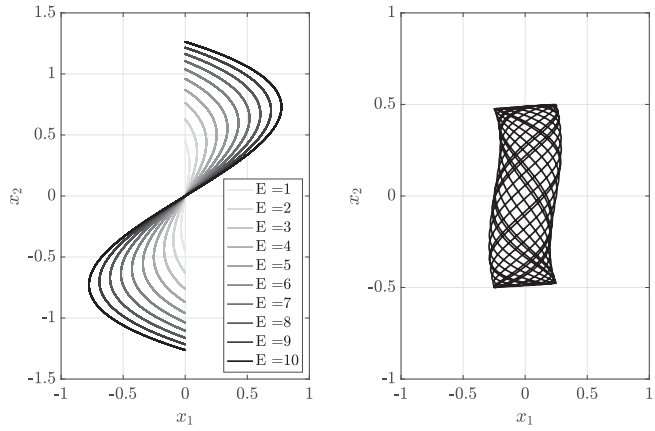

(a) Modal oscillations (b) $x(0) = (0.25, 0.5) \notin \mathfrak{M}$

Fig. 6. A collection of modal oscillations for system (21) are shown in Panel (a). As a comparison, Panel (b) shows the trajectory resulting from 60 seconds of simulations when the initial condition is selected outside the eigenmanifold (the configuration has zero velocity).

C. Simulations: Single Jump

Consider the nonlinear mechanical system described by

$$\begin{aligned} &\ddot{x}_1 + 7x_1 - 2x_2^3 = \tau_1, \\ &\left(10 + 3x_2^4\right)\ddot{x}_2 + 6\dot{x}_2^2 x_2^3 + x_2\left(3\,{x_2}^4 - 6\,x_1\,x_2 + 10\right) = \tau_2, \end{aligned} \quad (21)$$

with potential energy $V(x) = x_2^2\,(x_2^4 + 10)/2 - 2\,x_1\,x_2^3 + 7x_1^2/2$. The equilibrium is in (0,0), and the two eigenspaces of the linearized system are $\mathrm{Span}\{(1,0,0,0),(0,0,1,0)\}$ and $\mathrm{Span}\{(0,1,0,0),(0,0,0,1)\}$. The Eigenmanifold prolonging the second eigenspace (i.e. $x_{\mathrm{m}} = x_2$) is described by the embeddings $X(x_2, \dot{x}_2) = (x_2 \dot{x}_2^2, x_2)$, $\dot{X}(x_2, \dot{x}_2) = (\dot{x}_2^3 - 2x_2^2\dot{x}_2, \dot{x}_2)$.

We want to show here that Algorithm 1 succeeds in regulating a desired energy level while verifying (c2) and (2). Indeed, Fig. 6(a) shows a collection of modal oscillations across several energy levels. All intersect in the origin - making this an extended Rosenberg mode [4, Sec. IV]. Therefore, condition (13) is verified, and we can proceed by using impulses for actuation. This can be verified analytically by considering that $X(0, \dot{x}_2) = 0$ for all $\dot{x}_2$. However, this information is not explicitly inserted into the controller. This jumping point is autonomously found by Algorithm 1.

Also, to show the effectiveness of the decoupling between the two controllers, we consider here an Eigenmanifold stabilization loop $\tau_{\mathrm{c1}} = 2(\dot{x} - \dot{X})$ (see Sec. III and [24]). The system is initialized outside of the Eigenmanifold, and the jump is executed only after that the first loop has reached convergence. The desired energy level is $\bar{E} = 10$. The trajectory connected to the open loop evolution from this out-of-manifold initial condition is shown in Fig. 6(b), the closed loop trajectory in Fig. 7, and the corresponding time evolutions in Fig. 8. The system converges to $\mathfrak{M}$ in few seconds, and jumps around $t^* = 11$.

D. Multiple Jumps: A Preliminary Investigation of $\mathcal{R}^k$

If Algorithm 1 fails, we can safely assume that we cannot get from the given initial condition to the desired energy level with a single wait and jump sequence. Yet, we can use Algorithm 1

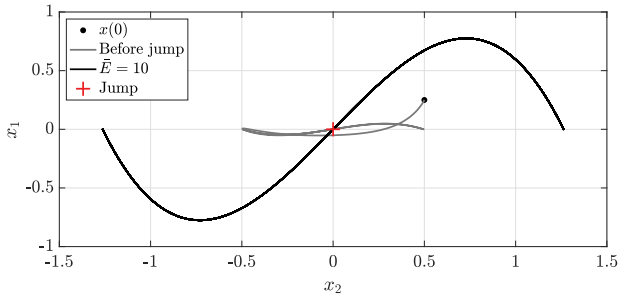

Fig. 7. Trajectories in configuration space, as a result of the application of Algorithm 1 and a transversal damping injection to (21). The system is initialized in $x(0) = (0.25, 0.5) \notin \mathfrak{M}$, and $\bar{E} = 10$. Note that the initial condition is the same of Fig. 6(b). The evolution from $x(0)$ to $\mathfrak{M}$ is shown in grey, the jump configuration in red, and the steady state modal trajectory in black - so to stress the transitions from one phase to the other.

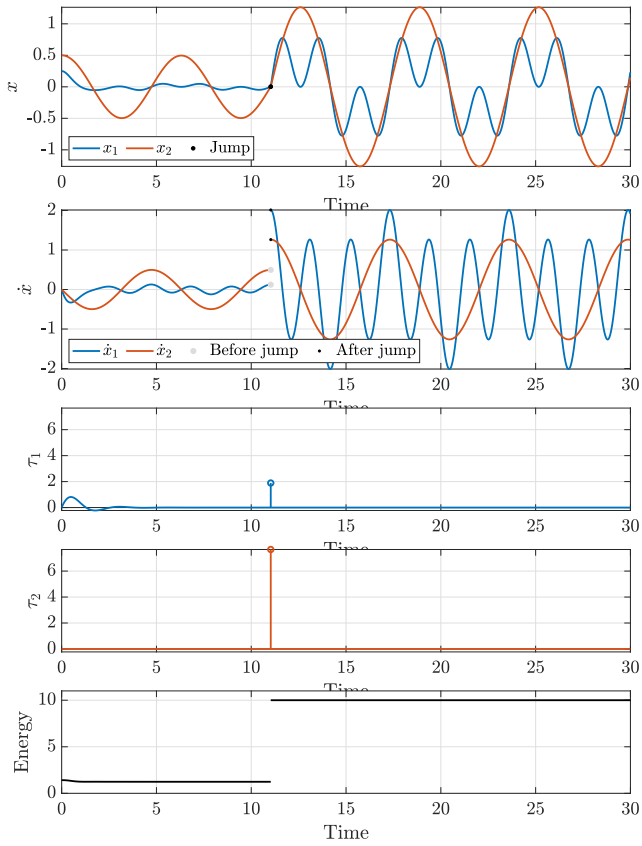

Fig. 8. Time evolutions of salient variables obtained as a result of the application of Algorithm 1 to system (21), With initial condition $x(0) = (0.25, 0.5) \notin \mathfrak{M}$, and $\bar{E} = 10$. Note that the initial condition is the same of Fig. 6(b). A single jump - happening around the eleventh second - is sufficient to reach the desired energy level.

as a building block of a Monte Carlo exploration, as proposed in Algorithm 2.

Corollary 2: If a subset of non null measure $\mathcal{E} \in \mathcal{P}(\mathbb{R}^{k-1})$ exists such that all elements in $\mathcal{E}$ define a feasible sequence of energy levels towards $\bar{E}$ then Algorithm 2 will converge in finite time returning an element of $\mathcal{E}$.

Proof: The thesis is proven by considering that if the measure of $\mathcal{E}$ is not null then the multivariate normal distribution generated by line 5 will eventually sample a sequence of energies from

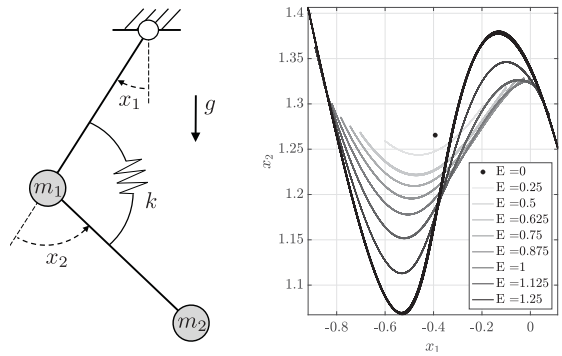

(a) Mechanical system (b) Modal evolutions

Fig. 9. A double pendulum with parallel elasticity acting on the second joint is depicted in Panel (a). Some modal trajectories part of the in-phase Eigenmanifold are shown in Panel (b). The trajectories do not self-intersect for low energies, but they do with (and at) higher energy. Also the points of crossing changes in number and in position depending on the energy level.

that set. Then Lemma 3 can be iteratively invoked to prove that each execution of oneJump will return the correct impulsive input. Note that the same Lemma also allows to prove that oneJump can be used to detect if the sample is inside or outside $\mathcal{E}$ (see lines 10 and 11). ■

E. Simulations: Double Pendulum With Parallel Elasticity

Consider the double pendulum in Fig. 9(a). The system is subject to gravity. Also, it has a linear spring connected in parallel to the second joint (stiffness k, and pre-load $\pi/2$). The two links have unitary length, and two masses m_1 and m_2 are connected at each end. The resulting inertia is $M_{1,1}(x_2) = m_1 + 2m_2(1 + \cos(x_2))$, $M_{2,1}(x_2) = m_2(1 + \cos(x_2))$, and $M_{2,2} = m_2$. The potential energy is $V(x) = V^*(x) - V^*(x_{\text{eq}})$ with $V^*(x) = k(x_2 - \pi/2)^2/2 + (m_1 + m_2)(1 - \cos(x_1)) + m_2(1 - \cos(x_1 + x_2))$. We consider $k = 10$, $m_1 = 0.4$, $m_2 = 0.4$. The equilibrium configuration is $x_{\text{eq}} = (-0.3930, 1.2655)$. We consider the Eigenmanifold $\mathfrak{M}$ prolonging the in-phase line mode $ES \simeq \text{Span}\{(0.99, 0.10, 0, 0), (0, 0, 0.99, 0.10)\}$. Note that this system has been discussed in detail in [4, Secs. VIII,IX], where also the Eigenmanifold is evaluated and depicted. We therefore point to that work for more details. Fig. 9(b) shows a collection of trajectories of modal oscillations.

Two points should be made here. First, X and $\dot{X}$ could not be obtained in closed form for this system. They are instead evaluated numerically through cubic local interpolation. This simulation serves therefore as a test of the theory in non ideal conditions. Second, at low energies the modal oscillations do not intersect with each other. Therefore exploring $\mathcal{R}^1$ is not enough. However, at higher energy the trajectories get more curved and start intersecting multiple low energy evolutions. Therefore, we use Algorithm 2, to explore $\mathcal{R}^2$. The results are shown in Figs. 10 and 11. The initial state is $x(0) \simeq (-0.0626, 1.3249)$, $\dot{x}(0) = (0, 0)$, which has energy 0.6 and modal coordinates $(x_{\text{m}}(0), \dot{x}_{\text{m}}(0)) \simeq (0.0741, 0)$. We ask the algorithm to jump to energy 0.7. The higher energy level 0.86 is identified as intermediate base between the two jumps, which are happening for t^* close to 3 and 7 seconds.

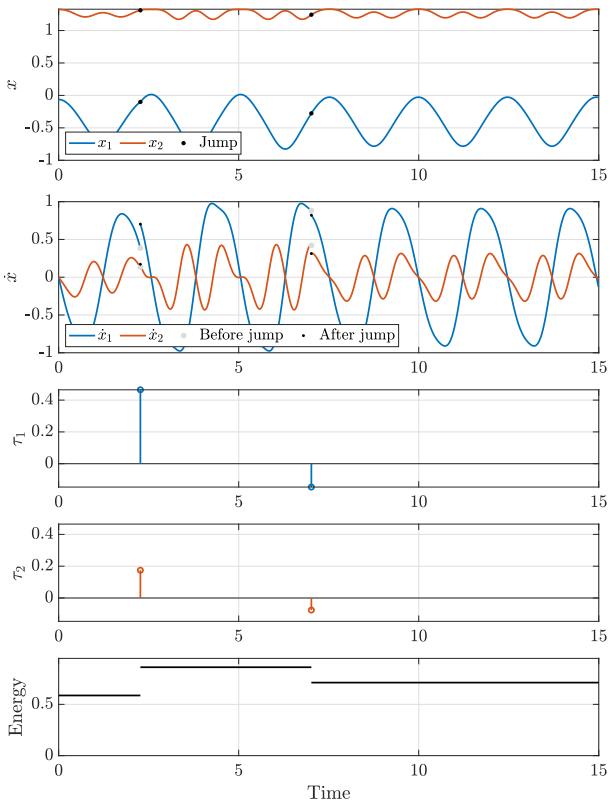

Fig. 10. Time evolutions of salient variables obtained as a result of the application of Algorithm 2 to a double pendulum with parallel elasticity, with $E^0 = 0.6$ and $\bar{E} = 0.7$ and $k = 2$. An intermediate mode which is part of $\mathcal{R}^1$ is identified with energy $E^1 = 0.86$. The two jumps happen around 3 and 7 seconds respectively.

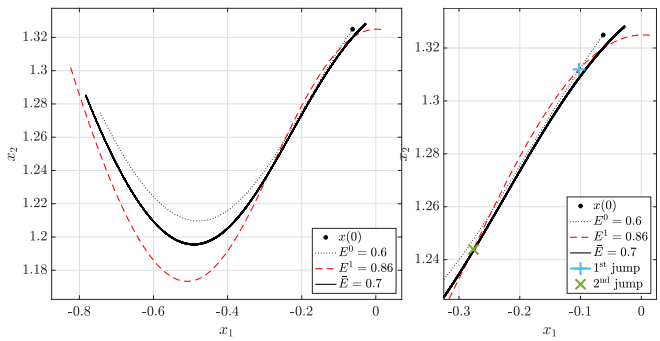

(a) Complete view (b) Zoom

Fig. 11. Trajectories in configuration space, as a result of the application of Algorithm 2 to a double pendulum with parallel elasticity. The three energy levels are plotted with different styles although resulting from a same evolution, in order to stress the transitions from one mode to the other.

VI. Discussion and Conclusions

We have proposed a classification of eigenmanifolds in three distinct classes, based on their projection in configuration space - as shown in Fig. 2. We have proven that to each class corresponds a fundamentally different actuation modality that can be exerted without pushing a system out of the eigenmanifold - namely bounded (Fig. 2(a)), impulsive (Fig. 2(b)), and no action (Fig. 2(c)). Based on this result, we have proposed control algorithms enabling the transitioning between two modal oscillations. Future work will be devoted to perform experiments, and extend the theory to non conservative and hybrid systems.

References

[1] B. Vanderborght *et al.*, "Variable impedance actuators: A review," *Robot. Auton. Syst.*, vol. 61, no. 12, pp. 1601–1614, 2013.
[2] L. F. van der Spaa, W. J. Wolfslag, and M. Wisse, "Unparameterized optimization of the spring characteristic of parallel elastic actuators," *IEEE Robot. Automat. Lett.*, vol. 4, no. 2, pp. 854–861, Apr. 2019.
[3] C. D. Santina, M. G. Catalano, and A. Bicchi, "Soft robots," in *Encyclopedia of Robotics*, M. H. Ang, O. Khatib, B. Siciliano, Eds., Berlin, Heidelberg: Springer, 2020, pp. 1–15. [Online]. Available: https://doi.org/10.1007/978-3-642-41610-1_146-2
[4] A. Albu-Schäffer and C. Della Santina, "A review on nonlinear modes in conservative mechanical systems," *Annu. Rev. Control*, vol. 50, pp. 49–71, 2020.
[5] M. Maggiore and L. Consolini, "Virtual holonomic constraints for euler-lagrange systems," *IEEE Trans. Autom. Control*, vol. 58, no. 4, pp. 1001–1008, Apr. 2013.
[6] G. Garofalo and C. Ott, "Passive energy-based control via energy tanks and release valve for limit cycle and compliance control," *IFAC-PapersOnLine*, vol. 51, no. 22, pp. 73–78, 2018.
[7] R. Ortega *et al.*, "Orbital stabilization of nonlinear systems via the immersion and invariance technique," *Int. J. Robust Nonlinear Control*, vol. 30, no. 5, pp. 1850–1871, 2020.
[8] B. Yi *et al.*, "Orbital stabilization of nonlinear systems via mexican sombrero energy shaping and pumping-and-damping injection," *Automatica*, vol. 112, 2020, Art. no. 108661.
[9] T. Marcucci *et al.*, "Parametric trajectory libraries for online motion planning with application to soft robots," *Robotic Research*. Cham, Switzerland: Springer, Nov. 2019, pp. 1001–1017, doi: 10.1007/978-3-030-28619-4_67.
[10] S. Haddadin *et al.*, "Optimal control for exploiting the natural dynamics of variable stiffness robots," in *Proc. IEEE Int. Conf. Robot. Automat.*, pp. 3347–3354, 2012.
[11] M. Uemura, H. Goya, and S. Kawamura, "Motion control with stiffness adaptation for torque minimization in multijoint robots," *IEEE Trans. Robot.*, vol. 30, no. 2, pp. 352–364, Apr. 2014.
[12] M. A. Hopkins *et al.*, "Compliant locomotion using whole-body control and divergent component of motion tracking," in *Proc. IEEE Int. Conf. Robot. Automat.*, pp. 5726–5733, 2015.
[13] M. Khoramshahi *et al.*, "Adaptive natural oscillator to exploit natural dynamics for energy efficiency," *Robot. Auton. Syst.*, vol. 97, pp. 51–60, 2017.
[14] F. Angelini, C. Petrocelli, M. G. Catalano, M. Garabini, G. Grioli, and A. Bicchi, "Softhandler: An integrated soft robotic system for the handling of heterogeneous objects," *IEEE Robot. Automat. Mag.*, vol. 27, no. 3, pp. 55–72, Sep. 2020.
[15] G. Kerschen *et al.*, "Nonlinear normal modes, Part I: A useful framework for the structural dynamicist," *Mech. Syst. Signal Process.*, vol. 23, no. 1, pp. 170–194, 2009.
[16] C. D. Santina and A. Albu-Schaeffer, "Exciting efficient oscillations in nonlinear mechanical systems through eigenmanifold stabilization," *IEEE Contr. Syst. Lett.*, p. 1, Dec. 2020, doi: 10.1109/LCSYS.2020.3048228.
[17] B. Bouchard *et al.*, "Optimal control of trading algorithms: A general impulse control approach," *SIAM J. Financial Math.*, vol. 2, no. 1, pp. 404–438, 2011.
[18] E. Verriest *et al.*, "Control of epidemics by vaccination," in *Proc. Amer. Control Conf.*, 2005, pp. 985–990.
[19] A. Koenig and S. D'Amico, "Fast algorithm for fuel-optimal impulsive control of linear systems with time-varying cost," *IEEE Trans. Autom. Control*, p. 1, Sep. 2020, doi: 10.1109/TAC.2020.3027804.
[20] T. Yang, *Impulsive Control Theory*. Berlin, Germany: Springer Science & Business Media, vol. 272, 2001.
[21] M. I. El-Hawwary and M. Maggiore, "Reduction theorems for stability of closed sets with application to backstepping control design," *Automatica*, vol. 49, no. 1, pp. 214–222, 2013.
[22] F. B. Mathis, R. Jafari, and R. Mukherjee, "Impulsive actuation in robot manipulators: Experimental verification of pendubot swing-up," *IEEE/ASME Trans. Mechatronics*, vol. 19, no. 4, pp. 1469–1474, Aug. 2014.
[23] D. Calzolari, C. D. Santina, and A. Albu-Schäffer, "Pd-like regulation of mechanical systems with prescribed bounds of exponential stability: The point-to-point case," *IEEE Contr. Syst. Lett.*, p. 1, Dec. 2020, doi: 10.1109/LCSYS.2020.3046538.
[24] C. D. Santina *et al.*, "Using nonlinear normal modes for execution of efficient cyclic motions in articulated soft robots," in *Proc. Int. Symp. Exp. Robot.*, 2021, vol. 19.